MADRID
inter.noise 2019
June 16 - 19
NOISE CONTROL FOR A BETTER ENVIRONMENT

Influence of uncertain parameters on the acoustic behaviour of sound proofing laminates

Gaborit, Mathieu[1]
LAUM UMR 6613, Le Mans Université, Avenue Olivier Messiaen, 72 085 CEDEX Le Mans, France
MWL, KTH Royal Institute of Technology, Teknikringen 8, SE10044, Stockholm, Sweden

Dazel, Olivier[2]
LAUM UMR 6613, Le Mans Université
Avenue Olivier Messiaen, 72 085 CEDEX Le Mans, France

Göransson, Peter[3]
MWL, KTH Royal Institute of Technology
Teknikringen 8, SE10044, Stockholm, Sweden

ABSTRACT

The protection against excessive noise has gathered a lot of attention along the years. Tailored solutions for specific types of noise conditions emerged and many communications on the subject are published every year. Although designing sound proofing systems is a well developed topic, building the proposed systems is still subject to many uncertainties. For instance, the very nature of the foams used in many broadband absorbers implies a degree of uncertainty on some of the most important parameters (e.g. the airflow resistivity). This phenomenon is even more noticeable in modern sound absorbing laminates in which every interface implies a barely controllable change in the continuity conditions. This effect being rarely accounted for and the interfaces' properties hard to quantify, it adds uncertainties that are widely neglected even though having a potentially strong impact.

In this contribution, the effect of randomly distributed parameters on the overall acoustic response of multi-layer systems is considered. The influence of choosing specific acoustic models for each layer is emphasized and the resulting response envelope is studied.

Keywords: uncertainty, acoustic absorbers, screens, poro-elastic materials
I-INCE Classification of Subject Number: 35
(see http://i-ince.org/files/data/classification.pdf)

[1]gaborit@kth.se
[2]olivier.dazel@univ-lemans.fr
[3]pege@kth.se

1. INTRODUCTION

As noise is a major annoyance for a large part of the population [8] the design of new soundproofing systems remains a prominent topic in engineering and research year after year.

In an engineering context, the designers have to devise a compromise between production costs, customers' expectations and legal regulations. Satisfying the last two points is not a trivial task even when reasonable requirements are set. Indeed, the most commonly used media for building sound packages (poro-elastic foams) are known for their variability. This phenomenon is observed as much between different batches and even at different locations on a single panel. Moreover, the standardised methods used to characterise the properties of poro-elastic media (PEM) are based on small-scale samples and usually lead to variable results depending on how the panel is sampled.

Admitting there's a number of uncertainties that can't be easily alleviated (in the characterisation & production stages), it is of interest to understand how the variability of parameters impacts the system's response.

The present contribution compares the effect of uncertainties on different parameters has on the simulated responses, accounting as well for different modelling strategies. The document is organized as follows. Section 2 introduces the physical and numerical models used to generate the results. Section 3 presents evidence that another technique than the Monte Carlo approach might be suitable to assess the variability of the response. Section 4 discusses the choice of the physical models for the films and its impact on the generated envelopes. An overall conclusion and some ideas for future works follow.

2. MODELS, METHODS AND MEDIA

This section briefly presents the numerical method used to generate the data for this paper as well as the underlying physical models. The system under study is composed of two layers of poro-elastic materials (PEM) backed by a perfectly rigid wall (see Figure 1).

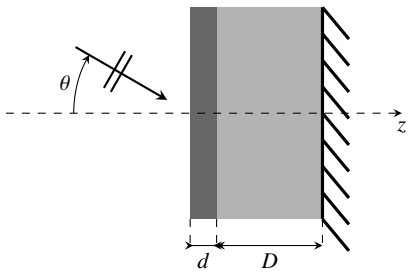

Figure 1: The system is composed of a PEM of thickness D bonded on a rigid wall topped by a thin film also porous (which thickness is denoted d).

The present contribution discusses the variability on the system's response to a plane wave excitation given an uncertainty on the flow resistivity σ of the film or its thickness d. Indeed, both these parameters are know to play a prominent role in the behaviour of the system [15]. In the present contribution the parameters are assumed to be normally distributed, centred on their "nominal" values. The standard deviation is determined by measurements performed on a set of film samples. These characterisations are beyond the scope of the present paper.

Table 1: Physical parameters of the foam and films used in the examples of sections 3 and 4. In the examples the thicknesses are chosen as $d = 1 \cdot 10^{-3}$ m and $D = 3 \cdot 10^{-2}$ m.

Parameters (unit)	Foam	Film a	Film b
ϕ	0.994	0.72	0.04
σ (N·s·m^{-4})	9045	$87{\cdot}10^3$	$775{\cdot}10^3$
$\tilde{\alpha}_\infty$	1.02	1.02	1.15
Λ' (μm)	197	480	230
Λ (μm)	103	480	230
ρ_1 (kg·m^{-3})	8.43	171	809
ν	0.42	0	0.3
E (Pa)	$194.9{\cdot}10^3$	$50{\cdot}10^3$	$260{\cdot}10^6$
η	0.05	0.5	0.5

2.2.1. Numerical model

The response of the system is computed using the recursive method proposed by Dazel *et al.* [5]. This formalism alleviates stability issues sometimes encountered with the more usual Transfer Matrix Method [10, 11], computing the transmission of the fields layer by layer instead of relying on a global approach. Details are given in the original paper [5] and a reference implementation is available online [9].

2.2.2. Physical models

Poro-elastic media are bi-phasic materials with complex interaction between the skeleton (solid phase) and the interstitial fluid. In the present contribution, the layers are modelled either as Biot materials (thus accounting for displacement fields in both phases) or as equivalent fluids (considering, in the present case, a very soft skeleton).

Biot model Following this first model, the evolution of the fields in the medium is described through a set of couple partial differential equations. Although the original theory used the solid- and fluid-borne displacements [1–3], the current contribution (as well as the numerical method) uses the total and solid phase displacements [6] with the motion equations:

$$\hat{\sigma}_{ij,j} = -\omega^2 \tilde{\rho}_s u_i^s - \omega^2 \tilde{\rho}_{eq} \tilde{\gamma} u_i^t, \qquad p_{,i} = \omega^2 \tilde{\rho}_{eq} \tilde{\gamma} u_i^s + \omega^2 \tilde{\rho}_{eq} u_i^t, \tag{1}$$

and the two constitutive laws:

$$\hat{\sigma}_{ij} = \hat{A} u_{i,i}^s \delta_{ij} + 2N\varepsilon_{ij}, \qquad p = -\tilde{K}_{eq} u_{i,i}^t. \tag{2}$$

In these equations, $\boldsymbol{u}^s$ and $\boldsymbol{u}^t$ are respectively the solid and total displacement fields, p is the interstitial pressure, $\hat{\boldsymbol{\sigma}}$ and $\boldsymbol{\epsilon}$ are the in-vacuo stress and strain tensors and δ_{ij} is the Kronecker symbol. Other variables are physical properties of the medium, representing densities ($\tilde{\rho}_{eq,s}$), compressibility ($\tilde{K}_{eq}$), Lamé coefficients ($\hat{A}$ and N) and a fluid/solid coupling term ($\tilde{\gamma}$).

Note that the equivalent parameters $\tilde{\rho}_{eq}$ and $\tilde{K}_{eq}$ are determined following the Johnson-Champoux-Allard model [1, 4, 12]. For the equivalent compressibility $\tilde{K}_{eq}$:

$$\tilde{K}_{eq} = \frac{\gamma_0 P_0}{\phi}\left[\gamma_0 - \frac{\gamma_0 - 1}{\tilde{\alpha}'}\right]^{-1}, \quad \tilde{\alpha}' = 1 + \frac{\omega'_\infty F'(\omega)}{2j\omega}, \quad F'(\omega) = \sqrt{1 + \frac{\mathrm{j}\omega}{\omega'_\infty}}, \quad \omega'_\infty = \frac{16\nu'_0}{\Lambda'^2} \tag{3}$$

with γ_0, ν_0 and P_0 being parameters of the air in the pores (resp. its polytropic coefficient, kinematic viscosity and atmospheric pressure). The coefficient Λ' corresponds to the thermal characteristic length, ϕ to the porosity and ω is the angular frequency.

And for the equivalent density $\tilde{\rho}_{eq}$:

$$\tilde{\rho}_{eq} = \frac{\rho_0 \alpha_\infty}{\phi}\left[1 + \frac{\omega_0}{\mathrm{j}\omega} F(\omega)\right], \quad \omega_0 = \frac{\sigma\phi}{\rho_0\alpha_\infty}, \quad F(\omega) = \sqrt{1 + \frac{\mathrm{j}\omega}{\omega_\infty}}, \quad \omega_\infty = \frac{1}{4\mu_0\rho_0}\left(\frac{\sigma\phi\Lambda}{\alpha_\infty}\right)^2 \tag{4}$$

where ρ_0 and μ_0 are the density and dynamic viscosity of the interstitial air, σ is the flow resistivity of the medium, Λ its viscous characteristic length and α_∞ is the high-frequency limit of its tortuosity.

This semi-phenomenological model can predict complex interactions between the phases but requires a lot of different parameters to be characterised. At the cost of some assumptions, simpler models have been developed which allow to represent specific types of media using less parameters.

Limp model Assuming its skeleton is very soft, the medium can be modelled as an equivalent fluid [6] with the following equivalent density $\tilde{\rho}_l$:

$$\tilde{\rho}_l = \tilde{\rho}_{eq}\left(\frac{\delta_{s1}}{\delta_{s2}}\right)^2, \quad \delta^2_{s1} = \frac{\omega^2\left(\tilde{\rho}_s - \tilde{\gamma}^2\tilde{\rho}_{eq}\right)}{\hat{A} + 2N}, \quad \delta^2_{s2} = \frac{\omega^2\tilde{\rho}_s}{\hat{A} + 2N} \tag{5}$$

The associated equivalent compressibility is the one proposed by Champoux and Allard [4] as presented in equation Equation 3. Note that other assumptions, not referenced herein, might lead to equivalent fluids models with different properties.

A note on empirical models The present contribution aims both at presenting a method to assess the effect of uncertain parameters and at discussing the differences resulting from the choice of physical model. For conciseness, this paper focuses on two widely-used models (Biot and limp) and overlooks another commonly used class of empirical models. Indeed, models such as those of Delany and Bazley [7] or Miki [14] do not embed the actual physical relations and it seems unreasonable to use them for uncertainty quantification.

3. FROM SAMPLES TO BOUNDS

In order to evaluate the response envelope of a system when a parameter is not known precisely, the most naive technique consists in computing the response for a large number of random samples from the said parameter's distribution. This approach relates to *Monte Carlo* techniques and is based on the assumption that combining a large number of samples will eventually lead to a good estimate of the true quantity [13]. Even though

this method is effective it might not be the most efficient when evaluating the model is costly.

The film are known to predominantly induce a pressure jump [15], thereby slightly changing the film's parameters is thought to have mostly an effect on the amplitude of the reflection/absorption coefficient. To try and simplify the envelope generation process, it is proposed to compare the so-called Monte Carlo envelope with the responses for specific values of a parameter ξ (bounds-envelope):

$$\xi^{\pm} = \bar{\xi} \pm n\hat{\xi} \tag{6}$$

where $\bar{\xi}$ represents the parameter's nominal value and $\hat{\xi}$ the associated standard deviation. The variable n is a real number (even if only integer cases are used here). Note that choosing $n = 1$, $n = 2$ or $n = 3$ corresponds to evaluating the bounds-envelopes for the 68%, 95% or 99.7% confidence intervals respectively In the present contribution, ξ refers either to the flow resistivity σ or to the film's thickness d.

In the following a specific representation is proposed to compare the different generated envelopes. The so-called *centred envelope* for the bounds-envelope for a given frequency response function R and a varying parameter ξ is computed as:

$$R(\bar{\xi} \pm n\hat{\xi}) - R(\bar{\xi}) \tag{7}$$

Note that in the case of the Monte Carlo results, one may compute the envelopes either by evaluating the sample-wise standard deviation (standard deviation envelope) or by using the two following curves (extremal envelope):

$$\min_S \Big(R_{MC}(f)\Big) - < R_{MC}(f) >_S \quad \text{and} \quad \max_S \Big(R_{MC}(f)\Big) - < R_{MC}(f) >_S \tag{8}$$

where $< \cdot >_S$ denotes the sample-wise average, and $\min_S$, $\max_S$ are the sample-wise maximum and minimum.

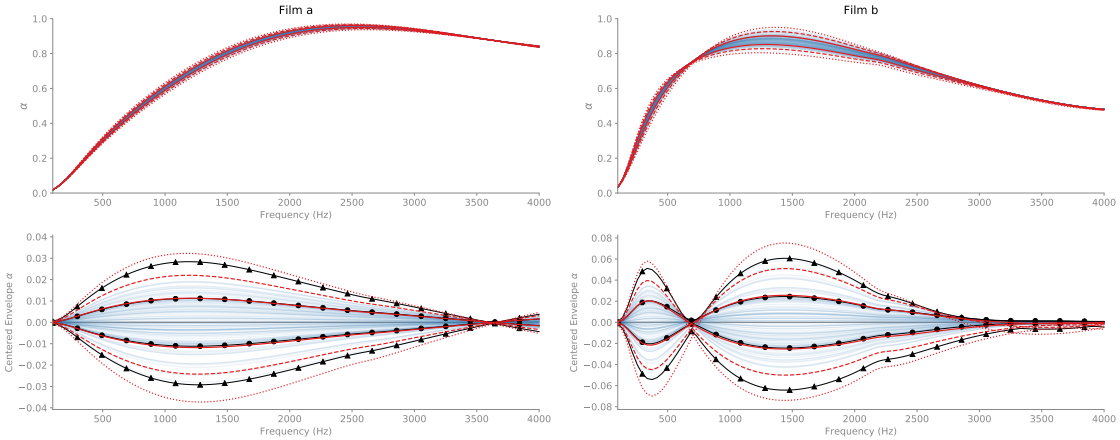

Figure 2: Comparison between Monte Carlo envelopes (draws in thin blue, standard deviation envelope with • and extremal envelope with ▲) and bounds-envelopes in red ($n = 1$ in solid lines, $n = 2$ in dashed lines and $n = 3$ in dotted lines). For two different films with parameters presented in Table 1 at normal incidence ($\theta = 0$) for a 10% deviation of σ in the film.

The comparison is shown in figure 2 and one sees that the bounds-envelopes match their Monte-Carlo equivalent closely. The standard deviation envelope from the Monte

Carlo results fits the $n = 1$ curve as expected given the normal distribution's properties. The extremal envelope lies between the $n = 2$ and $n = 3$ curves that both follow the trend of the Monte Carlo envelope. The reason why there is no perfect match is that the number of draws in the Monte Carlo computation isn't large enough to completely cover the range of variation.

These results support the claim that for some parameters (in the present case σ), the costly Monte Carlo procedure can be replaced by a few computations at specific values of the variation interval. This reduces the cost of computing the envelopes but requires that this technique is tested for each and every varying parameter.

4. ENVELOPES' FEATURES

In Figures 3 and 4 the bounds-envelopes ($n = 1$) for different varying parameters (the film's flow resistivity σ on Figure 3 and its thickness d on 4) are computed for two different films (parameters in Table 1) are compared to the Monte Carlo standard deviation envelopes. Especially, this figures displays the envelopes generated for 2 different physical models for the film (Biot and Limp).

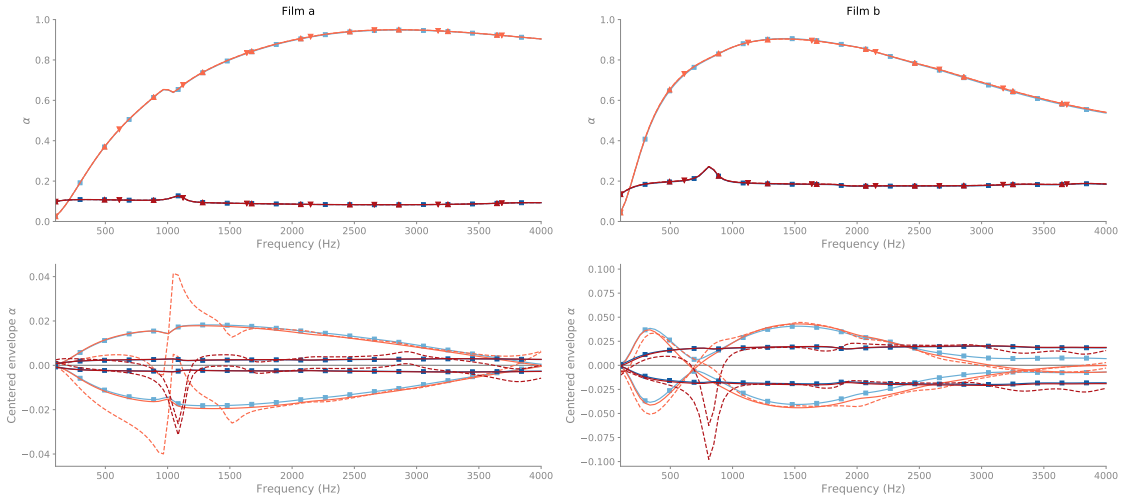

Figure 3: Influence of the model choice for a 10% standard deviation on the film's flow resistivity σ.
Top: average curve for a Monte Carlo resolution (in blue solid lines) and the nominal curves for two different physical models in the film (Biot in solid lines with ▲ markers and Limp with dashed lines and ▼ markers). Bottom: Centred envelopes generated for the different models: Monte-Carlo standard deviation in blue, bounds-envelopes with Biot model in solid red lines with ▲ markers and bounds-envelope with Limp model in dashed red lines with ▼. Generated for the two films presented in Table 1 and two angles ($\theta = 30$ deg in light colours and $\theta = 89$ deg, grazing incidence, in darker shades).

First of all, it seem that the average and nominal curves computed with the different models (shown on the upper part of the figures) agree over the whole frequency band and for both films and both angles.

It's seen as well that the bounds-envelopes generated using a Biot model closely follow the Monte Carlo reference over the whole frequency band. This is not the case for the Limp model that diverges around resonances. Even though seemingly equivalent for the nominal curve, choosing a Biot or a Limp model for the film (while keeping the

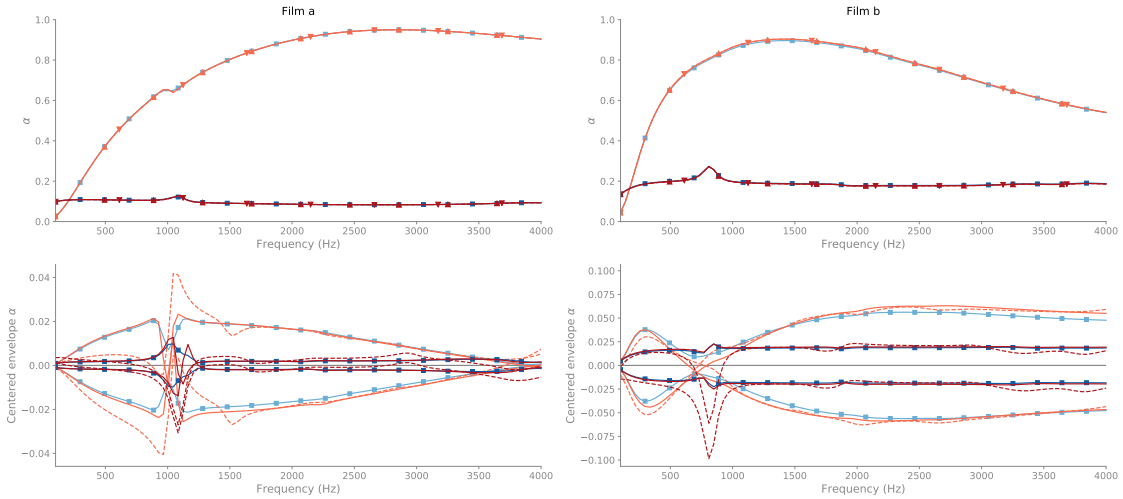

Figure 4: Influence of the model choice for a 10% standard deviation on the film's thickness d.
Top: average curve for a Monte Carlo resolution (in blue solid lines) and the nominal curves for two different physical models in the film (Biot in solid lines with ▲ markers and Limp with dashed lines and ▼ markers). Bottom: Centred envelopes generated for the different models: Monte-Carlo standard deviation in blue, bounds-envelopes with Biot model in solid red lines with ▲ markers and bounds-envelope with Limp model in dashed red lines with ▼. Generated for the two films presented in Table 1 and two angles ($\theta = 30$ deg in light colours and $\theta = 89$ deg, grazing incidence, in darker shades).

rest untouched) results doesn't allow reconstructing a envelope whereas choosing a Biot model does.

The envelopes generated using the Monte Carlo approach or the bounds approach with a Biot model for the film show an interesting effect: they tend to collapse at specific frequencies. In figure 5, the centred bounds-envelopes are computed up to 10kHz and it is seen that they seem to have periodic constrictions, and even complete collapses at given frequencies. For the higher part of the spectrum, this can be linked to modes in the absorber however, the collapses/constrictions lower in frequency remain to be investigated.

5. CONCLUSION

Considering envelopes in place of single "nominal" curves gives a better representation of reality. Indeed the components of modern absorbers have an important parameters variability that might impact the full system's properties. This has to do with the characterisation techniques used to determine the properties: relying on a few small-sized samples, the reported values might not always represent perfectly the media under study.

The present contributions shows that Monte Carlo is not the only viable method to determine the envelopes and that simpler models (such as Limp) might be used over part of the frequency band to analyse the effects. Understanding what causes the constrictions might be a way to understand how interactions are accounted for by the different models and how it might impact the quantification of uncertainties.

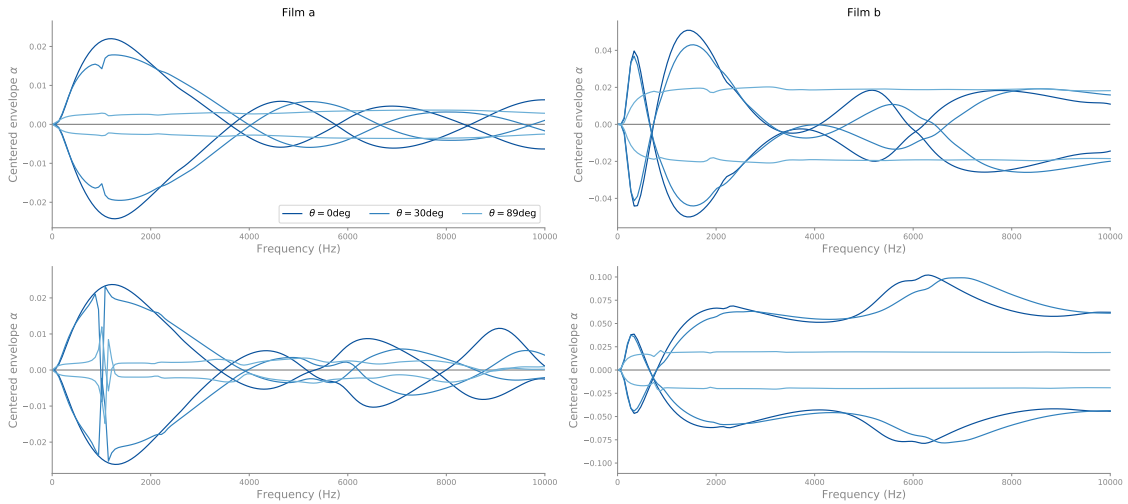

Figure 5: Centred envelope generated using the bounds methods with the film modelled as a Biot material over a large frequency band for three different incidence angles (0, 30 and 89 deg *from the darkest to the lightest) and two different films. Top: assuming a 10% standard deviation on the film's flow resistivity σ and, Bottom: assuming a 10% standard deviation on the film's thickness.*

6. REFERENCES

References

[1] J.-F. Allard and Noureddine Atalla. *Propagation of Sound in Porous Media: Modelling Sound Absorbing Materials*. 2nd. Hoboken, N.J: Wiley, 2009. 358 pp.

[2] M. A. Biot. Theory of Propagation of Elastic Waves in a Fluid-Saturated Porous Solid. *The Journal of the Acoustical Society of America*, 28(2):168, 1956. DOI: 10.1121/1.1908239.

[3] M. A. Biot and D. Willis. The Elastic Coefficients of the Theory of Consolidation. *Journal of Applied Mechanics*, 1957.

[4] Yvan Champoux and Jean-F. Allard. Dynamic Tortuosity and Bulk Modulus in Air-Saturated Porous Media. *Journal of Applied Physics*, 70(4):1975, 1991. DOI: 10.1063/1.349482.

[5] O. Dazel et al. A Stable Method to Model the Acoustic Response of Multilayered Structures. *Journal of Applied Physics*, 113(8):083506, 2013. DOI: 10.1063/1.4790629.

[6] Olivier Dazel et al. An Alternative Biot's Displacement Formulation for Porous Materials. *The Journal of the Acoustical Society of America*, 121(6):3509, 2007. DOI: 10.1121/1.2734482.

[7] M. E. Delany and E. N. Bazley. Acoustical Properties of Fibrous Absorbent Materials. *Applied acoustics*, 3(2):105–116, 1970.

[8] European Environment Agency. *Managing Exposure to Noise in Europe*. Jan. 2017.

[9] Mathieu Gaborit and Olivier Dazel. Pymls: Multilayer Solver in Python for Acoustic Problems, Feb. 2019. DOI: 10.5281/zenodo.2558137.

[10] N. A. Haskell. The Dispersion of Surface Waves on Multilayered Media*. *Bulletin of the Seismological Society of America*, 43(1):17–34, Jan. 1, 1953.

[11] Bernard Hosten and Michel Castaings. Transfer Matrix of Multilayered Absorbing and Anisotropic Media. Measurements and Simulations of Ultrasonic Wave Propagation through Composite Materials. *The Journal of the Acoustical Society of America*, 94(3):1488–1495, Sept. 1993. DOI: 10.1121/1.408152.

[12] David Linton Johnson, Joel Koplik, and Roger Dashen. Theory of Dynamic Permeability and Tortuosity in Fluid-Saturated Porous Media. *Journal of fluid mechanics*, 176(1):379–402, 1987.

[13] Malvin H. Kalos and Paula A. Whitlock. *Monte Carlo Methods*. 2., rev. and enl. ed. OCLC: 254048500. Weinheim: WILEY-VCH, 2008. 203 pp.

[14] Yasushi Miki. Acoustical Properties of Porous Materials-Modifications of Delany-Bazley Models. *Journal of the Acoustical Society of Japan (E)*, 11(1):19–24, 1990.

[15] Allan D. Pierce. *Acoustics: An Introduction to Its Physical Principles and Applications*. 1989th ed. Woodbury, N.Y: Acoustical Society of America, 1989. 678 pp.